Journal of Thermal Analysis and Calorimetry, Vol. 84 (2006)1, 157–163

EVALUATION OF POZZOLANIC ACTIVITY AND PHYSICO-MECHANICAL CHARACTERISTICS IN METAKAOLIN-LIME PASTES

A. Bakolas, E. Aggelakopoulou, A. Moropoulou and S. Anagnostopoulou*

National Technical University of Athens, School of Chemical Engineering, Section of Materials Science and Engineering
9 Iroon Polytechniou St., 15773 Zografou, Athens, Greece

In order to evaluate the pozzolanic activity of metakaolin, several pastes were prepared, by mixing metakaolin with hydrated lime, in different ratios. The pastes were stored in standard conditions (*RH*=99±1%, *T*=25±1°C) and evaluated using thermal analysis (DTA/TG), X-ray diffraction (XRD), compressive strength tests and mercury intrusion porosimetry (MIP), in time. The obtained results revealed that the compounds formed are CSH, C_2ASH_8 and $C_4A\bar{C}H_{11}$ while C_4AH_{13} was not detected up to 270 days of curing. The calcium hydroxide consumption increases as the initial amount of the metakaolin in the paste augments. The maximum strength development is obtained for metakaolin/lime ratio:1.

Keywords: *hydration phases, lime, metakaolin, pozzolanic activity, thermal analysis*

Introduction

Metakaolin ($Al_2Si_2O_7$ or AS_2) is a high active aluminosilicate material which is formed by the dehydroxylation of kaolin ($Al_2(OH)_4Si_2O_5$) precursor upon heating in the ~700–800°C temperature range [1]. The pozzolanic activity of a material is defined as its ability to react with portlandite ($Ca(OH)_2$), in the presence of water [2]. The pozzolanic activity depends on a number of factors, the most significant of which seem to be the chemical and mineralogical composition of the additive, the amorphous phase content, the dehydroxylation degree, the specific surface area, the $Ca(OH)_2$ content in the paste, the admixture content and the water to binder ratio in the material [3, 4].

During the last decade, several studies have been accomplished regarding the metakaolin-cement-water system [5] while a few research works concern the metakaolin-lime-water pastes [6–8]. The prime objective of these works was the characterization of the compounds formed when metakaolin (MK) reacts with calcium hydroxide. Frias and Cabrera have studied the effect of temperature in compounds formed in MK-lime pastes cured at 20°C (up to 360 days of hydration) [6] and at 60°C [7]. Obtained results revealed that CSH, C_2ASH_8 (strätlingite) and C_4AH_{13} were formed in the case of pastes stored at 20°C, whereas at 60°C C_3AH_6 (hydrogarnet) was also detected.

Most of the works published up to now about MK/lime system are focused on reaction kinetics. However, there is scant information about the MK-lime pastes' microstructure and mechanical characteristics; although the pore size distribution has been studied in MK-OPC pastes [9–11].

In order to study the development of hydration phases of MK-lime system, pastes with different mixing ratio of MK-lime were prepared, cured at 20°C, up to 270 days of hydration. The compounds formed were defined using DTA/TG and XRD analysis, while the pastes' microstructure and mechanical characteristics are determined using mercury intrusion porosimetry and mechanical tests. The study of MK/lime system could provide us valuable information regarding the acquired mechanical strength and the hydration products formed in the case of MK/lime mortars addressed to historic buildings' restoration interventions.

Materials and methods

Several pastes were prepared, by mixing metakaolin (MK) – Metastar 501 of IMERYS Minerals Ltd. – with powder commercial hydrated lime (L), in different MK/lime ratio. Table 1 reports the chemical composition and the physical properties of the materials used for the pastes preparation. Regarding the hydrated lime, DTA/TG analysis revealed that the contained percentage of $Ca(OH)_2$ is ~89%, while the relevant percentage of $CaCO_3$ arises to ~5%.

The grain size distribution of metakaolin was determined by laser particle size analyzer (CILAS 715). It presents a great fineness with cumulative passing per-

* Author for correspondence: amoropul@central.ntua.gr

1388–6150/$20.00

Akadémiai Kiadó, Budapest, Hungary
Springer, Dordrecht, The Netherlands

Table 1 Chemical analysis and physical properties of materials used in pastes preparation

MT	SiO_2/ %	Al_2O_3/ %	Fe_2O_3/ %	CaO/ %	MgO/ %	K_2O/ %	Na_2O/ %	SO_3/ %	LOI/ %	$d_{app.}$/ g cm^{-3}	d_{real}/ g cm^{-3}	A_s/ m^2 g^{-1}
L	0.17	0.18	0.07	70.06	2.35	–	–	0.77	25.60	0.50	2.34	13.60
MK	51.70	40.60	0.64	0.71	0.96	2.00	0.31	0.10	1.19	0.38	2.52	13.83

MT: Material, LOI: Loss of ignition, $d_{app.}$ /g cm^{-3}: apparent density according to EN-45, d_{real}/g cm^{-3}): real density according to ASTM C-188-95, A_s/m^2 g^{-1}): Specific surface area-BET method

centage at 24 and 16 μm up to 100.0 and 95.6% correspondingly. X-ray diffraction analysis revealed that metakaolin is comprised by mica, quartz and feldspar.

Regarding the pozzolanic activity of MK, the percentages of total silica and active silica (according to EN 197-1 and EN 196-2) were determined as 54.19 and 44.59%, respectively. Finally, the pozzolanicity of metakaolin (according to Greek Presidential Decree 244/1980, article 8) is determined up to 13.1 MPa.

Table 2 reports the mass ratios of the various components employed for pastes' preparation. The mixing procedure was the same for all pastes: first, the amount of lime was mixed with the total amount of water, it was stirred for 3 min in a mixer and afterwards the metakaolin was added gradually in the paste and it was stirred for other 20 min. The pastes were casted in cubic moulds of 2×2×2 cm and minicylinders (diameter: 2 cm, height: 4 cm [12]) and stored in standard conditions (*RH*=99±1%, *T*=25±1°C). The samples were demolded after 3 days of hydration and stored in the same conditions till the testing date.

The following techniques were used for the evaluation of physicochemical and mechanical characteristics of pastes:

- Differential Thermal and Thermogravimetric Analysis (DTA/TG - Netzsch 409EP) in a static air atmosphere with heating rate of 10°C min^{-1} from ambient temperature up to 1000°C, in order to investigate the $Ca(OH)_2$ consumption and to determine the pozzolanic reaction products in time. DTA/TG measurements were performed at 3, 7, 14, 28, 90 and 270 days of curing time, on ~100 mg of powder. Before each collection of DTA/TG samples from the cube, the first 4–5 mm of the surface was removed by grinding, afterward they were placed in an oven at 60°C for 2 h and then in a desiccator for 1 h. Moreover, DTA/TG was performed on samples, taken just after pastes production and following the pre-mentioned samples preparation. These measurements are indicated as 0 days.
- X-Ray Diffraction Analysis (XRD, Siemens D-500) for the identification of crystalline compounds in pastes at different ages (0, 3, 7, 14, 28, 90 and 270 days). The preparation of XRD samples was the same as the DTA/TG one.
- Mechanical test performed in minicylinders, for the compressive strength and elastic modulus of elasticity determination, at 30 and 90 days of curing time (Wykeham Farrance, load cell: 50 KN, loading rate: 0.1 mm min^{-1}).
- Mercury Intrusion Porosimetry (MIP, Fisons, Porosimeter 2000) for the microstructural characteristics determination at 90 days of curing time. Before each collection of MIP samples from the cube, the first 4–5 mm of the surface was removed by grinding and the samples were stored in a desiccator for 48 h.

Table 2 Ratio of MK/L and Water/(L+MK) (per mass) used for pastes preparation

Paste	MK/Lime	Water/(L+MK)
MK05	0.5	1.00
MK1	1	1.00
MK2	2	1.00

Results and discussion

Differential thermal and thermogravimetric analysis (DTA/TG)

DTA curve of MK is shown in Fig. 1. Only one sharp exothermic peak could be noticed at ~985°C, attributed to the formation of 'precursors' (γ-alumina or aluminum-silicon spinel and amorphous silicate) of high-temperature phases (mullite and cristobalite) [13–15]. Furthermore, the temperature of this exothermic peak could be shifted to lower temperature for a poorly-crystallized kaolinite [13].

Figures 2–4 report the DTA curves of MK05, MK1, MK2 pastes at 0, 3, 7, 14, 28, 90 and 270 days of curing. The main endothermic (endo) and exothermic (exo) peaks are observed in the following temperature ranges:

- 120–145°C (endo) Dehydration of CSH
- 180–200°C (endo) Dehydration of C_2ASH_8 (strätlingite or gehlenite hydrate)
- 490–525°C (endo) Dehydration of $Ca(OH)_2$
- 720–760°C (endo) Decarbonation of $CaCO_3$
- 940–970°C (exo) 'Precursors' of mullite and cristobalite.

It should be noticed that the peak concerning the dehydration of CSH is slightly shifted to higher temperatures (from 120 to 145°C) for 0 to 28 days of aging while beyond this period the temperature of the peak is decreasing. Regarding the peak attributed to strätlingite, it is shifted to higher temperatures from 180 to 200°C for 0 to 270 days.

The characteristic peak of CSH dehydration is rather broad until 7 days of curing time and narrow beyond 7 and 14 days for MK05 and MK1, MK2 respectively. In addition, this peak seems to be sharpest for 28 days whereas exhibits a lower intensity beyond this period.

Regarding the endotherm at 180–200°C, attributed to gehlenite hydrate, it is firstly detected for all pastes at 3 days and it seems to be quasi broader in time. Also, in this temperature range and more specifically at ~160–220°C, the dehydration of $C_4A\overline{C}H_{11}$ ($3CaO\cdot Al_2O_3\cdot CaCO_3\cdot 11H_2O$, monocarboaluminate) occurs [16–18]. Therefore an overlapping with the peak of C_2ASH_8 should be occurred. Though, the presence of monocarboaluminate is confirmed by XRD analysis.

The intensity of the endotherm attributed to $Ca(OH)_2$(CH) dehydration is reduced, in time, while for MK1 and MK2 the free CH is totally consumed at 14 and 7 days, respectively.

In almost all curves an exothermic peak at ~980°C with insignificant mass loss on TG is observed. This peak is, also, detected in the case of pure metakaolin as mentioned above. For MK05 this peak is noticed till 14 days of aging and it disappears beyond this period, since the total amount of metakaolin is consumed. On the other hand, for MK1 and MK2 this peak could be detected till 270 days due to the existence of 'free' metakaolin in the paste.

It is worth to notice that hydrogarnet is not detected up to 270 days, indicating that this compound is associated with high curing temperatures [6].

The results of this investigation present some differences with the results referred in the literature. More specifically, it was stated that the compounds formed in MK/lime pastes cured at 20°C are CSH, C_2ASH_8 and C_4AH_{13} [6] while in this study no C_4AH_{13} was detected up to 270 days. On the contrary, $C_4A\overline{C}H_{11}$ is detected in this study, fact that is ascribed to the presence of $CaCO_3$ in the lime used for pastes' preparation.

By using TG/DTG analysis as long as the 2nd derivative of DTA [19] the mass loss (%) of the chemical compounds detected in pastes are calculated and presented in Figs 5–7 for MK05, MK1 and MK2 respectively, *vs*. curing time. All pastes present low percentage of physically absorbed water (calculated from 25 up to 100°C), less than 1%. In addition for all pastes, it is observed mass loss attributed to dehydration of CSH (calculated from 100°C to the end of phenomenon) is formed at 0 day and exhibits a maximum value at the age of 28 days. Beyond this period a significant decrease is discerned up to 270 days.

Mass loss concerning the C_2ASH_8 and the $C_4A\overline{C}H_{11}$ ($(H)_{str.+mca.}$), presents an increase till 270 days of curing time where the maximum value is detected. Moreover, the mass loss attributed to the residual chemical bound water ($(H)_{r.ch.b.}$), is calculated from the end of gehlenite hydrate dehydration up to the beginning of calcium hydroxide dehydration is reported [20]. These values present an increasing trend with curing for all pastes.

Regarding, the free CH, it is consumed at 14 and 7 days for MK1 and MK2 whereas percentage of free

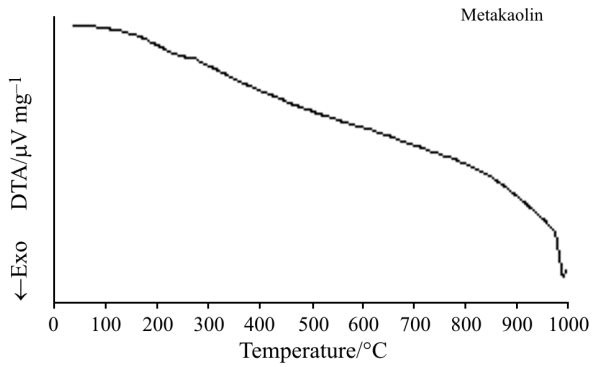

Fig. 1 DTA curve of MK

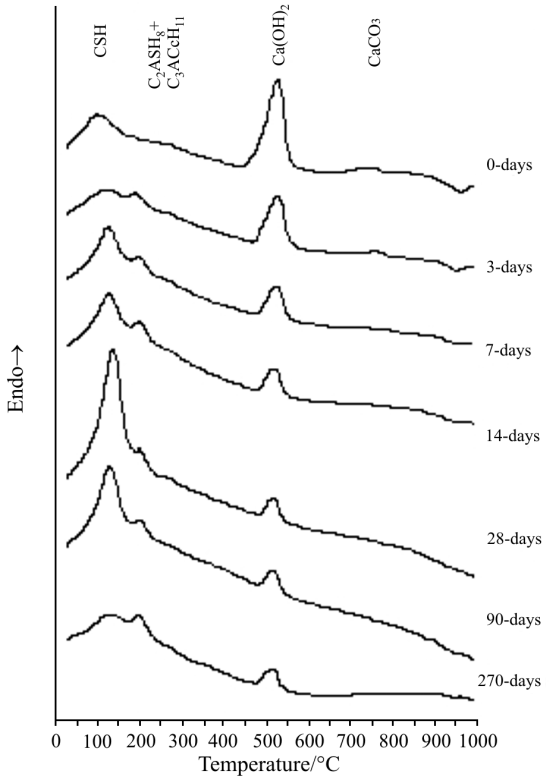

Fig. 2 DTA curves for MK05

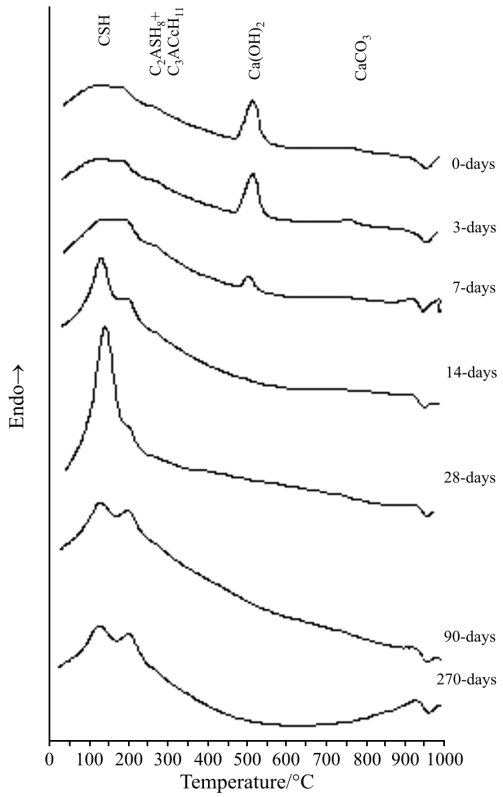

Fig. 3 DTA curves for MK1

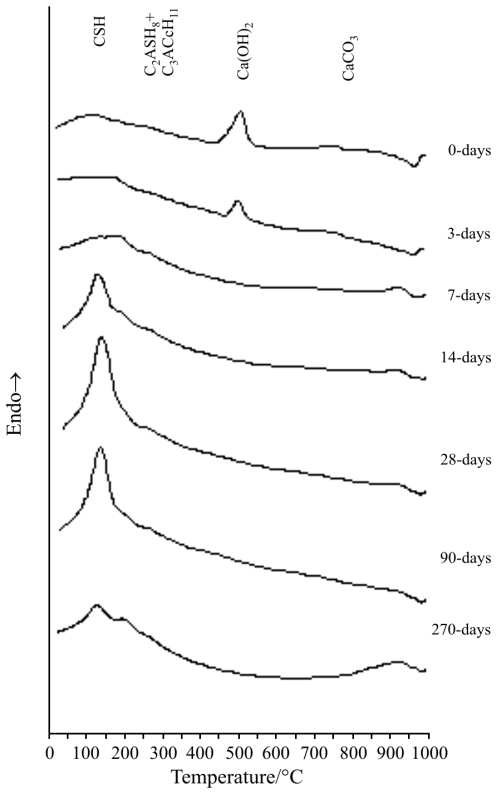

Fig. 4 DTA curves for MK2

CH remains in MK05. The mass loss ascribed to $CaCO_3$ present insignificant variations in time.

The mass loss attributed to the total chemically bound water ($(H)_{t.ch.b.}$) is calculated according to the equation:

- $(H)_{t.ch.b.}=(H)_{CSH}+(H)_{str.+mca}+(H)_{r.ch.b.}$
- $(H)_{t.ch.b.}$: Total chemical bound water, calculated in the temperature range ~100–460°C
- $(H)_{CSH}$: Chemical bound water of CSH, calculated in the temperature range ~100–160°C
- $(H)_{str.+mca}$: Chemical bound water of strätlingite and monocarboaluminate, calculated in the temperature range ~160–230°C
- $(H)_{r.ch.b.}$: Residual chemical bound water, calculated in the temperature range ~230–460°C

For all pastes, the total chemical bound water values present an increase till 28 days of aging and beyond this period a significant decrease is discerned up to 270 days.

Furthermore, taking into account the TG results, the percentage of consumed $Ca(OH)_2$ ($(CH)_{cons}$ (%)) is determined according to the Eq. [21]:

$$(CH)_{(cons.)}(\%)=100\frac{(CH)_0-(CH)_t}{(CH)_0} \qquad (21)$$

where: $(CH)_{(cons.)}$: consumed CH (%) at a specific age (t), $(CH)_0$: the initial amount of CH in the lime-metakaolin paste, $(CH)_t$: the amount of CH in the paste for a specific age (t).

Figure 8 presents $(CH)_{cons}$ (%) *vs.* curing age for MK05, MK1, MK2 pastes. From the results, it is noticed that the highest rate of CH consumption is reported for MK2, followed by MK1 and MK05. For MK1 and MK2 the whole amount of free CH is consumed after 28 and 7 days of curing, respectively. In the case of MK05, the rate of CH consumption presents high values till 7 days, it slows down beyond this period till 28 days and it remains stable up to 270 days. The $(CH)_{cons}$ (%) is about 73% at 270 days.

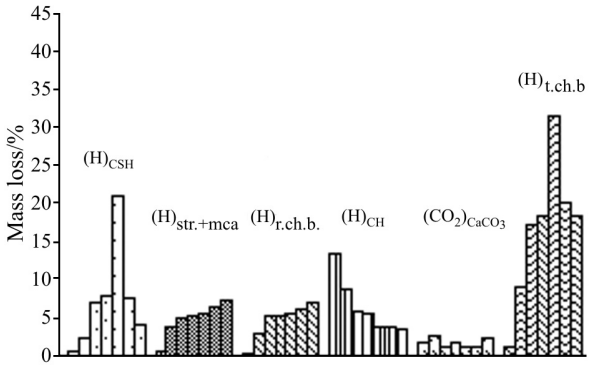

Fig. 5 Mass loss/% of the compounds detected in MK05 paste, at 0, 3, 7, 14, 28, 90, 270 days of curing time

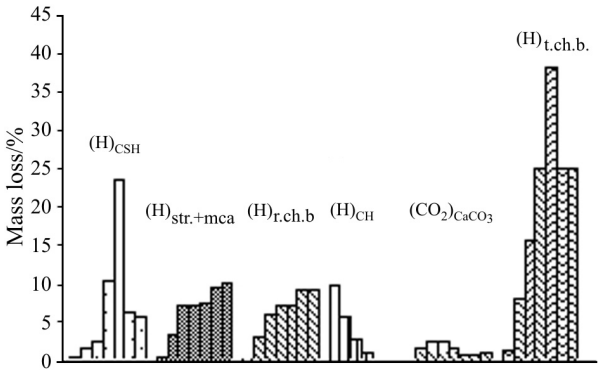

Fig. 6 Mass loss/% of the compounds detected in MK1 paste, at 0, 3, 7, 14, 28, 90, 270 days of curing time

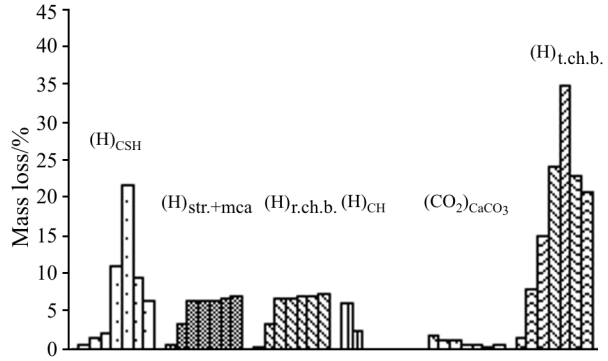

Fig. 7 Mass loss/% of the compounds detected in MK2 paste, at 0, 3, 7, 14, 28, 90, 270 days of curing time

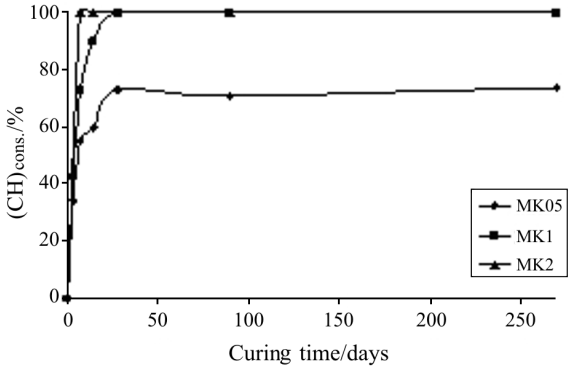

Fig. 8 Consumed CH (%) in time for MK05, MK1 and MK2

X-ray diffraction analysis (XRD)

Figure 9 illustrates the XRD patterns for MK pastes in different ages. At 0 days, only the patterns of portlandite (*P*) and calcite (*CC*) are noticed, attributed to the presence of lime in pastes. The intensity of these lines is decreased with time, as the reaction among lime and metakaolin is taking place. In the case of MK1 and MK2, no patterns of lime are detected at 14 and 7 days, correspondingly. This fact is in accordance with DTA/TG results.

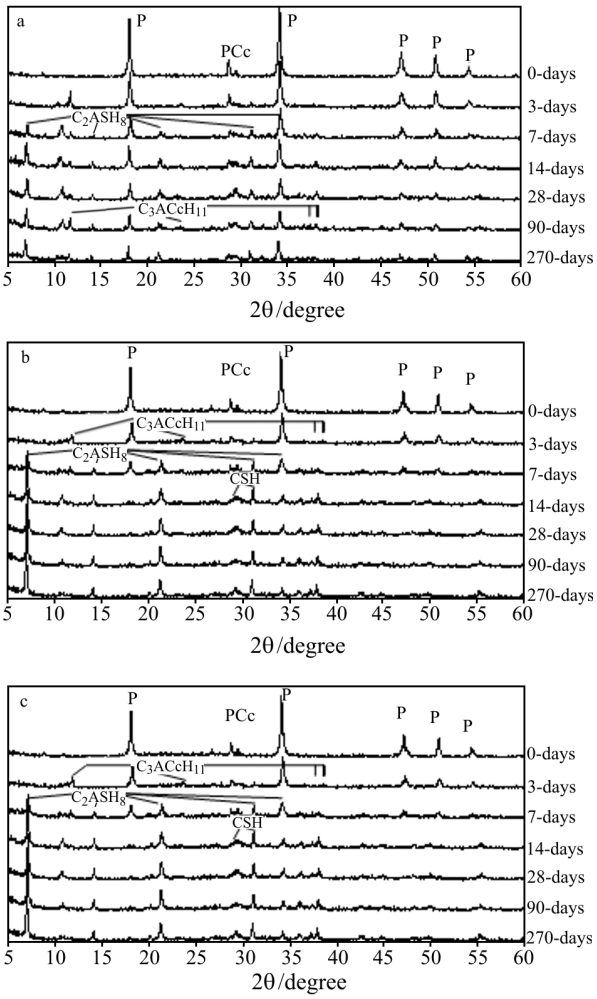

Fig. 9 XRD patterns for MK/lime pastes at 0, 3, 7, 14, 28, 90, 270 days of curing time a – MK05, b – MK1, c –MK2 (P: Portlandite, Cc: Calcite)

The patterns of hydrated products of pozzolanic reaction that have been detected by DTA/TG (CSH, C_2ASH_8) are also detected by XRD.

Strätlingite is not detected at 3 days of curing age, probably due to its low degree of crystallinity at that age. It is initially observed at 7 days for all pastes, with increasing intensity with time, especially for pastes produced with higher MK/lime ratio. For MK1 and MK2, strätlingite appears as the predominant phase beyond 7 days.

In addition, monocarboaluminate ($C_4A\overline{C}H_{11}$) is revealed beyond 3 days of curing time, as a result of reaction between CH and MK according to the following Eq. [18]:

$$AS_2+5CH+CC+8H \rightarrow C_4A\overline{C}H_{11}+2C–S–H$$

The patterns attributed to monocarboaluminate are more intense in the case of MK05, since the percentage of lime and therefore the *CC* content is higher than the other pastes. The intensity of this line de-

creases with time and at age of 270 days, it is slightly noticed. In the case of MK1 and MK2, $C_4A\overline{C}H_{11}$ is clearly detected from 3 to 14 days but beyond 14 days is not observed in X-ray diffractograms.

Moreover, CSH is hardly to be detected by X-ray analysis, due to its low degree of crystallinity. Nevertheless, in diffractograms of all pastes obtained, a wide band of peaks appears in the range of 2θ 28–31° [22], further than 7 days, attributed to the presence of CSH. At last, no C_4AH_{13} was detected, finding that is in accordance with DTA/TG results.

Mechanical tests

Table 3 presents the values of compressive strength performed on minicylinders (mean value of three measurements) as far as the values of static modulus of elasticity, calculated at 40% of the compressive strength (tangent E_{st}). Standard deviations of the three measurements are reported as well.

Table 3 Compressive strength and static modulus of elasticity for MK/lime pastes, at 30 and 90 days of curing time

Paste	Time/ days	F_c/ MPa	SD	$E_{st.}$/ MPa	SD
MK05	30	7.22	0.84	165	33
	90	7.96	0.95	258	19
MK1	30	12.26	1.50	385	35
	90	14.32	1.36	410	24
MK2	30	10.70	1.16	186	38
	90	11.23	1.32	395	45

F_c/MPa: Compressive strength, E_{st}/MPa: Static elastic modulus of elasticity, SD: Standard deviation

According to the obtained results, MK1 presents the highest values of compressive strength, followed by MK2 and MK05. Mechanical strength is increased slightly from 30 to 90 days for all pastes. This fact is not in accordance with the values of total chemical bound water that decreases for all pastes after 28 days (TG data). On the other hand a slight increase is observed to the mass loss values correspondent to strätlingite and monocarboaluminate as far as to the residual bound water, from 28 to 90 days.

Regarding the static modulus of elasticity, it can be noticed that it displays similar trend with compressive strength with maximum value reported for MK1 and MK2 pastes.

Mercury Intrusion Porosimetry (MIP)

Table 4 reports the microstructural characteristics of pastes (mean values of three measurements) at 90 days of curing time. It could be observed that the pore radius average presents the same values for MK1 and MK2, whereas MK05 exhibits higher one. As the ratio MK/lime increases, the open total porosity decreases. Similar trend is observed for corrected bulk density and total cumulative volume of pastes. Regarding the specific surface area, it presents almost the same values for MK05 and MK1 and much lower for MK2.

Figure 10 presents the distribution of specific volume ($mm^3\ g^{-1}$) to the pores radius of pastes where a different distribution could be noticed. MK05 exhibits a distribution shifted to coarser pores. Furthermore as the MK/lime ratio increases, there is a clear shift in the distribution to narrower pores. In addition, the curve correspondent to MK05 presents an increasing trend, fact that is probably attributed to the presence of narrower pores, beyond the detection of the instrument. In the case of MK1 this increasing trend is slighter whereas the slope of the curve attributed to MK2 remains stable.

Figure 11 presents the percentage of relative volume in different ranges of pore radius. It could be noticed that the higher percentage of relative volume is distributed in the range of pore radius 0.01–0.05 μm for all pastes. More specifically, the ~52, ~90, ~91% of the relative volume is distributed in this range of pores, for MK05, MK1 and MK2, correspondingly. In the case of MK05, the percentage of relative volume ascribed to pores in the range of 0.05–0.1 and 0.1–0.5 arises up to 20 and 19%, respectively.

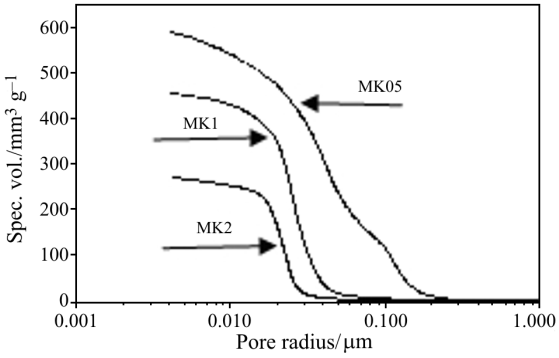

Fig. 10 Distribution of specific volume (mm^3/g) to the pore radius

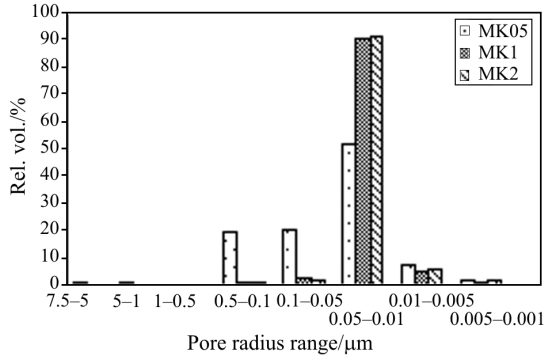

Fig. 11 Distribution of relative volume (%) in different ranges of pore radius

Table 4 Characteristics of pastes microstructure at 90 days of curing time as determined by Mercury Intrusion Porosimetry

Paste	T.C.V./mm^3 g^{-1}	A_s/m^2 g^{-1}	P.R.A./μm	d_{bulk}/g cm^{-3}	$d_{bulk.cor.}$/g cm^{-3}	O.T.P./%
MK0.5	589.0	44.64	0.037	0.98	2.32	57.7
MK1	454.6	43.05	0.024	1.07	2.08	48.6
MK2	271.3	30.19	0.024	1.19	1.76	32.3

T.C.V.: Total Cumulative Volume/mm^3 g^{-1}, A_s: Specific surface area /m^2 g^{-1}, P.R.A.: Pore Radius Average/μm, d_{bulk}: Bulk density/g cm^{-3}, $d_{bulk.cor.}$: Corrected bulk density/g cm^{-3}, O.T.P.: Open Total Porosity/%

Conclusions

From the obtained results the following conclusions could be drawn:

- DTA and XRD data revealed that the compounds formed during the pozzolanic reaction in MK/lime pastes are: CSH, C_2ASH_8 and $C_4A\overline{C}H_{11}$; no C_4AH_{13} was detected up to 270 days of curing, although this compound is referred in the literature, as a product of MK/lime pastes cured at 20°C.
- Regarding the lime consumption, the 100% of initial amount of calcium hydroxide is consumed after 28 and 7 days of curing for pastes of metakaolin/lime ratio of 1 and 2 respectively. For the paste prepared with the minor quantity of metakaolin, this percentage remains stable from 28 to 270 days.
- Mechanical strength is increased slightly from 30 to 90 days for all pastes. Static modulus of elasticity displays similar trend. The maximum value of compressive strength and static modulus of elasticity is reported for paste prepared by equal quantities of metakaolin and lime.
- As the metakaolin/lime ratio increases, the pastes' total cumulative volume and total porosity decrease and a clear shift in pore size distribution curve to narrower pores is observed. The higher percentage of relative volume is distributed in the pore radius between 0.01 and 0.05 μm.

References

1 D. S. Klimesch and A. Ray, Thermochim. Acta, 307 (1997) 167.
2 A. Shvarzman, K. Kovler, G. S. Grader and G. E. Shter, Cem. Concr. Res., 33 (2003) 405.
3 A. Shvarzman, K. Kovler, I. Schamban, G. S. Grader and G. E. Shter, Adv. Cem. Res., 14 (2002) 35.
4 W. Roszczynialski, J. Therm. Anal. Cal., 70 (2002) 387.
5 B. B. Sabir, S. Wild and J. Bai, Cem. Concr. Compos., 23 (2001) 441.
6 M. Frias and J. Cabrera, Cem. Concr. Res., 31 (2001) 519.
7 M. Frias Rojas and M. I. Sanchez de Rojas, Cem. Concr. Res., 33 (2003) 643.
8 J. Cabrera and M. Frias, Cem. Concr. Res., 31 (2001) 177.
9 M. Frias and J. Cabrera, Cem. Concr. Res., 30 (2000) 561.
10 J. M. Khatib and S. Wild, Cem. Concr. Res., 26 (1996) 1545.
11 M. Frías Rojas and M. I. Sánchez de Rojas, Cem. Concr. Res., 35 (2005) 1292.
12 S. Salvador, Cem. Concr. Res., 25 (1995) 102.
13 V. Balek and M. Murat, Thermochim. Acta, 282/283 (1996) 385.
14 M. C. Mayoral, M. T. Izquierdo, J. M. Andres and B. Rubio, Thermochim. Acta, 373 (2001) 173.
15 T. Mohammadi and A. Pak, Sep. Purif. Technol., 30 (2003) 241.
16 P. Ubbriaco and F. Tasselli, J. Therm. Anal. Cal., 52 (1998) 1047.
17 P. Bruno, D. Calabrese, M. Di Pierro, A. Genga, C. Laganare, D. A. P. Manigrassi, A. Traiani and P. Ubbriaco, Thermochim. Acta, 418 (2004) 131.
18 J. Pera and A. Amrouz, Adv. Cem. Based Mater., 7 (1998) 49.
19 D. S. Klimesch and A. Ray, Thermochim. Acta, 307 (1997) 167.
20 D. S. Klimesch and A. Ray, Thermochim. Acta, 306 (1997) 159.
21 J. Paya, J. Monzo, M. V. Borrachero, S. Velazquez and M. Bonilla, Cem. Concr. Res., 33 (2003) 1085.
22 P. Ubbriaco, P. Bruno, A. Traini and D. Calabrese, J. Therm. Anal. Cal., 66 (2001) 293.

DOI: 10.1007/s10973-005-7262-y